J Electroceram (2009) 23:542–547
DOI 10.1007/s10832-008-9531-1

One step synthesis and densification of nanocrystalline $TaSi_2$–Si_3N_4 composite from mechanically activated powders by high-frequency induction-heated combustion

Hyun-Kuk Park · Jeong-Hwan Park · Jin-Kook Yoon · Ki-Tae Lee · In-Jin Shon

Received: 28 May 2007 / Accepted: 18 June 2008 / Published online: 9 July 2008

Abstract Dense nanocrystalline $4TaSi_2$–Si_3N_4 composite was synthesized by high-frequency induction-heated combustion synthesis (HFIHCS) method within 1 min in one step from mechanically activated powders of TaN and Si. Simultaneous combustion synthesis and densification were accomplished under the combined effects of an induced current and mechanical pressure. Highly dense $4TaSi_2$–Si_3N_4 composite with relative density of up to 99% was produced under simultaneous application of a 60 MPa pressure and the induced current. The average grain size and mechanical properties (hardness and fracture toughness) of the composite were investigated.

Keywords High-frequency induction heated combustion · Composite materials · Sintering · Nanophase · Mechanical properties · $TaSi_2$–Si_3N_4

1 Introduction

High melting point intermetallic compounds with low density and improved oxidation resistance have received wide attention as potential aerospace materials over the past 20 years. In this regard, transition-metal silicides are very attractive for application temperature up to 1300 °C and higher because this class of materials has an attractive combination of properties, including high melting temperature, high modulus, high oxidation resistance in air, and a relatively low density [1, 2]. In addition, the thermal and electrical conductivities are relatively high and therefore they are also attractive for electronic interconnections and diffusion barriers. Most of the investigations on silicides have focused on a few compounds, with $MoSi_2$ and $TiSi_2$ being the most studied. Other silicides, such as $TaSi_2$, WSi_2, $NbSi_2$, $ZrSi_2$ and VSi_2 have received relatively little attention. The melting point, crystal structure, density, formation enthalpy at 298K, and adiabatic temperature of $TaSi_2$ are 2025 °C, hexagonal, 9.205 g/cm^3, 32.4 kJ mol^{-1}, and 1,795 K [3–5]. As in the case of many intermetallic compounds, the current concern about these materials focuses on their low fracture toughness below the ductile–brittle transition temperature [6–8]. To improve on their mechanical properties, the approach commonly utilized has been the addition of a second phase to form composites [9–14]. An example is the addition of Si_3N_4 to $TaSi_2$ to improve the latter's properties. Silicon nitride has a high thermal shock resistance, due to its low thermal expansion coefficient, and a good resistance to oxidation when compared to other structural materials [15, 16]. The isothermal oxidation resistance of $NbSi_2$–40 vol% Si_3N_4 composite prepared by spark plasma sintering (SPS) process in dry air at 1300 °C was superior to that of monolithic $NbSi_2$ compact since the composite contained a larger amount of Si, which made it easier to form dense SiO_2 scale [17]. Therefore, Si_3N_4 may be the most promising additive as a reinforcing material for $TaSi_2$-based composites.

H.-K. Park · J.-H. Park · K.-T. Lee · I.-J. Shon (✉)
Division of Advanced Materials Engineering,
Research Center of Industrial Technology,
Chonbuk National University,
664-14 Deokjin-dong 1-ga, Deokjin-gu, Jeonju,
Jeonbuk 561-756, Republic of Korea
e-mail: ijshon@chonbuk.ac.kr

J.-K. Yoon
Advanced Functional Materials Research Center,
Korea Institute of Science and Technology,
P.O Box 131, Cheongryang, Seoul 130-650, Republic of Korea.

Many similar high-temperature dense composites are usually prepared in a multi-step process [18, 19]. However, the method of field-activated and pressure-assisted combustion synthesis has been successfully employed to synthesize and densify materials from the elements in one step in a relatively short period of time. This method has been used to synthesize a variety of ceramics and composites, including $MoSi_2$–ZrO_2, Ti_5Si_3 and its composites, WSi_2 and its composites, and WC–Co hard materials [20–25]. These materials, which are generally characterized by low adiabatic combustion temperature, cannot be synthesized directly by the self-propagating high-temperature synthesis (SHS) method. More recently, a new approach has been developed in which synthesis and densification can be effected simultaneously. This new process, referred to as the high-frequency induction-heated combustion synthesis (HFIHCS), has been successfully used to synthesize and densify materials in one step in a relatively short period of time (2 min) [26–28].

The objective of this study is to investigate the preparation of dense nanocrystalline $4TaSi_2$–Si_3N_4 composite by the HFIHCS method starting from a mixture of mechanically activated TaN and Si powders. The interaction between these phases, i.e.,

$$4TaN + 11Si \rightarrow 4TaSi_2 + Si_3N_4$$

is thermodynamically feasible, as can be seen in Fig. 1.

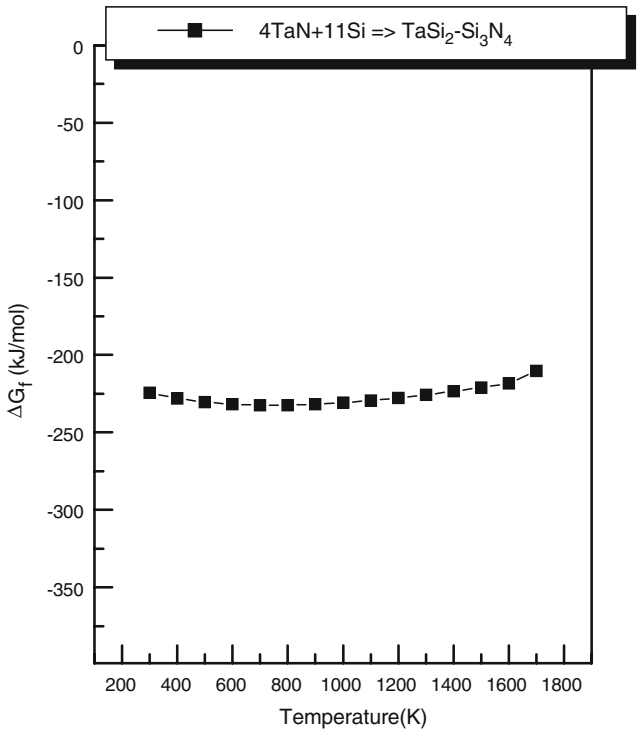

Fig. 1 Temperature dependence of the Gibbs free energy for the interaction between TaN and silicon

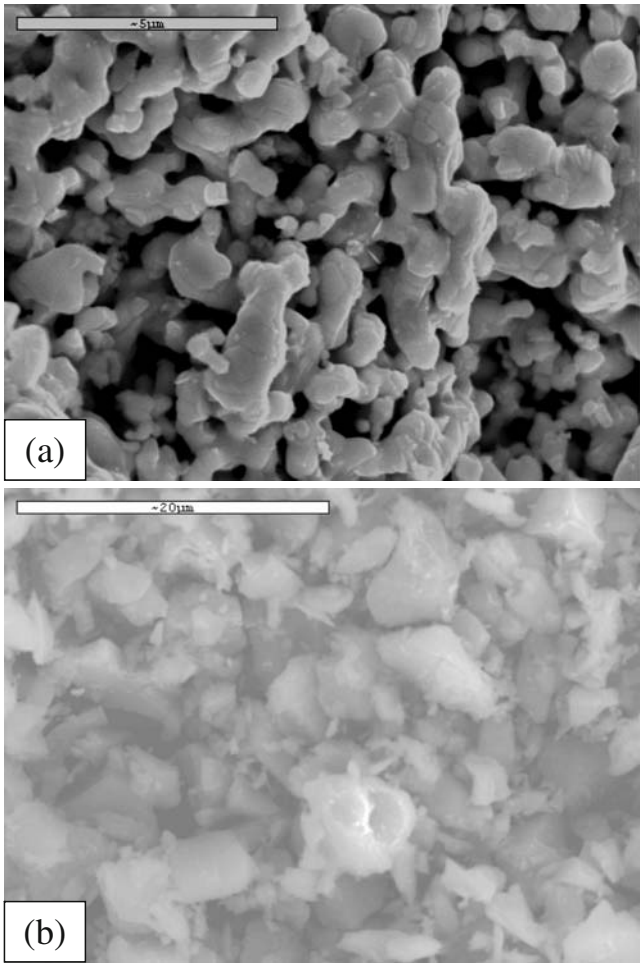

Fig. 2 Scanning election microscope images of raw materials: (**a**) tantalum nitride, (**b**) silicon

2 Experimental procedure

Powders of 99.5% tantalum nitride (−325 mesh, Alfa Products, Ward Hill, MA) and 99.5% pure silicon (−325 mesh, Alfa Products, Ward Hill, MA**)** were used as starting materials. Figure 2 shows the SEM images of the raw materials used. Powder mixtures of TaN and Si in the molar proportion of 4:11 were first milled in a high-energy ball mill (Pulverisette-5, planetary mill) at 250 rpm for 10 h. Tungsten carbide balls (5 mm in diameter) were used in a sealed cylindrical stainless steel vial under argon atmosphere. The weight ratio of ball-to-powder was 30:1. Milling resulted in a significant reduction of grain size. The grain size and the internal strain were determined by XRD analysis.

After milling, the mixed powders were placed in a graphite die (outside diameter, 45 mm; inside diameter, 20 mm; height, 40 mm) and then introduced into the high-frequency induction-heated combustion system, shown schematically in Fig. 3. Following the introduction of the die into the apparatus, the system was evacuated and a

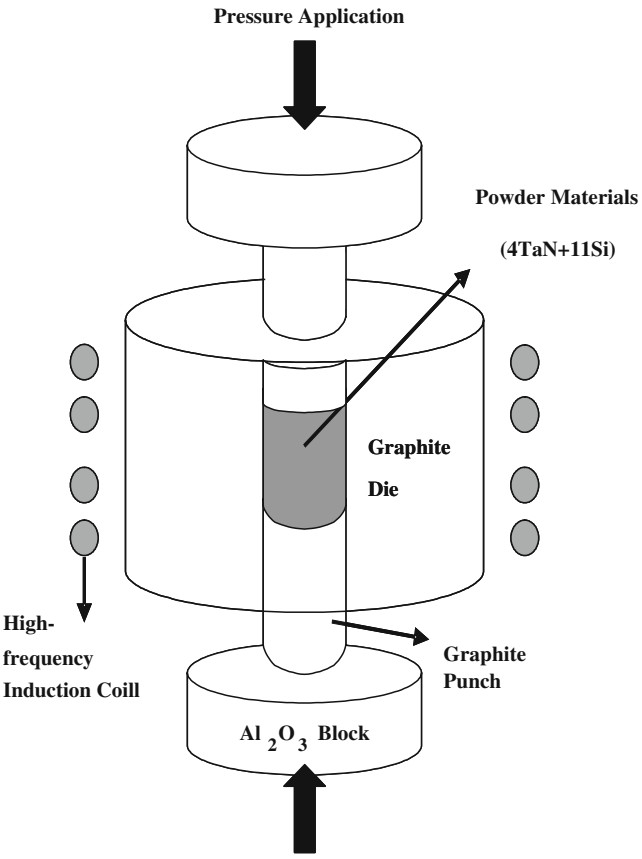

Fig. 3 Schematic diagram of the high-frequency induction heated combustion apparatus

uniaxial pressure of 60 MPa was applied. An induced current (frequency of about 50 kHz) was then activated and maintained until densification was attained as indicated by a linear gauge measuring the shrinkage of the sample. Temperatures were measured by a pyrometer focused on the surface of the graphite die. At the end of the process, the sample was cooled to room temperature. The process was carried out under a vacuum of 40 mTorr.

The relative densities of the synthesized sample were measured by the Archimedes method. Microstructural characterization was made on product samples which had been polished and etched using a solution of HF (30 vol.%), HNO_3 (30 vol.%) and H_2O (40 vol.%) for 8 s at room temperature. Compositional and microstructural analyses of the products were made through X-ray diffraction (XRD) and scanning electron microscopy (SEM) with energy dispersive X-ray analysis (EDAX). Vickers hardness was measured by performing indentations at a load of 10 kg and a dwell time of 15 s.

3 Results and discussion

Figure 4 shows XRD patterns of the raw powders and the milled 4TaN+11Si powder mixture. The FWHM of the

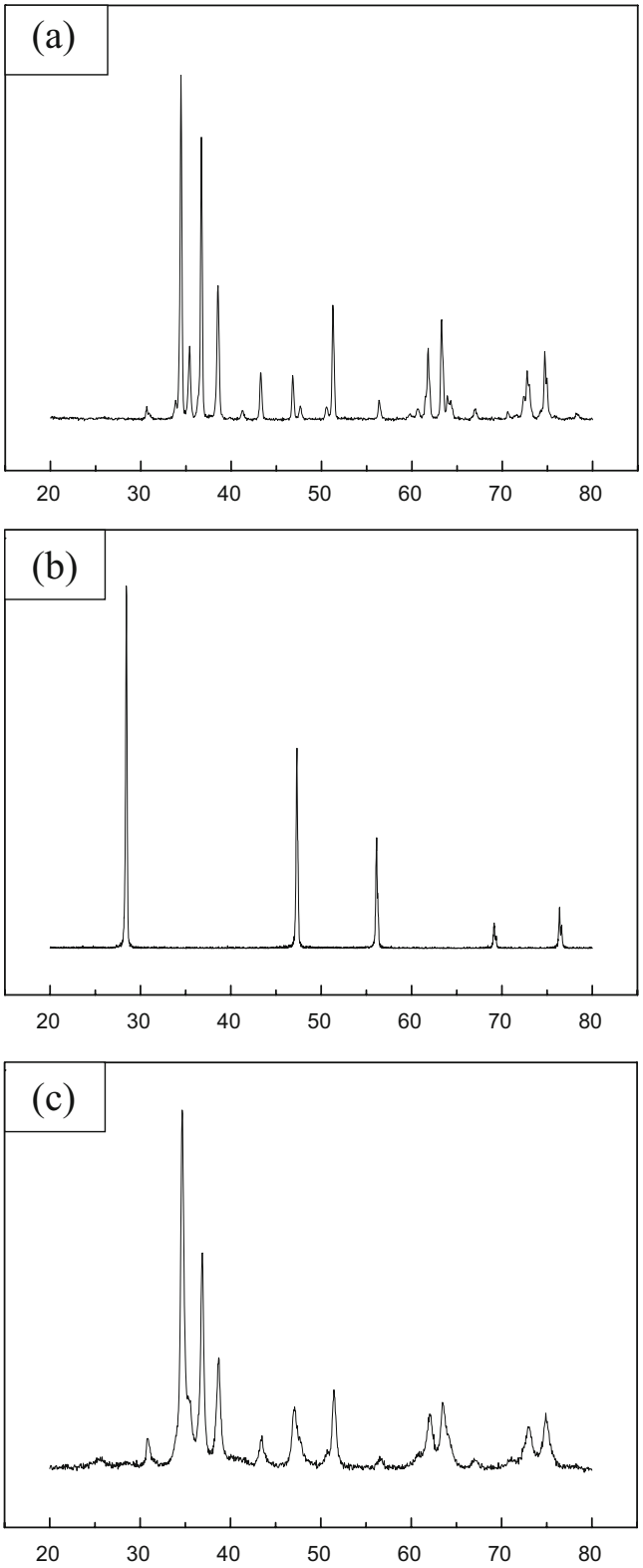

Fig. 4 XRD patterns of raw materials: (**a**) TaN, (**b**) Si and (**c**) milled 4TaN+11Si

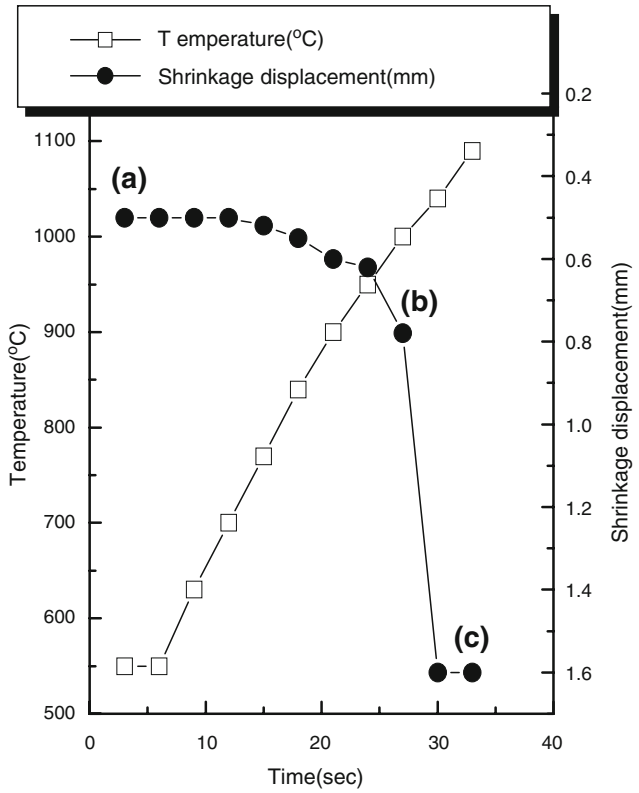

Fig. 5 Variations of temperature and shrinkage displacement with heating time during high-frequency induction heated combustion synthesis and densification of $4TaSi_2$–Si_3N_4 composite (under 60 MPa, 90% output of total power capacity)

milled powder is greater than that of the raw powders due to internal strain and grain size reduction. The grain size and the internal strain can be calculated by Stoke and Wilson's formula [29],

$$b = b_d + b_e = k\lambda/(d\cos\theta) + 4\varepsilon\tan\theta \quad (1)$$

where b is the full width at half-maximum (FWHM) of the diffraction peak after instrument correction; b_d and b_e are FWHM caused by small grain size and internal strain, respectively; k is constant (with a value of 0.9); λ is wavelength of the X-ray radiation; d and ε are grain size and internal strain, respectively; and θ is the Bragg angle. The parameters b and b_s follow Cauchy's form with the relationship: $B_0 = b + b_s$, where B_0 and b_s are FWHM of the broadened Bragg peaks and the standard sample's Bragg peaks, respectively.

The calculated average grain sizes and internal strains of the milled TaN and Si powders are 68 and 37 nm, 0.004 and 0.002, respectively.

The variations in shrinkage displacement and temperature with heating time during the processing of 4TaN+11Si system are shown in Fig. 5. As the induced current was applied, the shrinkage displacement increased gradually with temperature up to about 950 °C, but then abruptly increased at about 1000 °C. When the reactant mixture of 4TaN+11Si was heated under 60 MPa pressure to 950 °C, no reaction took place and no significant shrinkage displacement as judged by subsequent XRD and SEM analyses. Figure 6(a), (b), and (c) show the SEM (second-

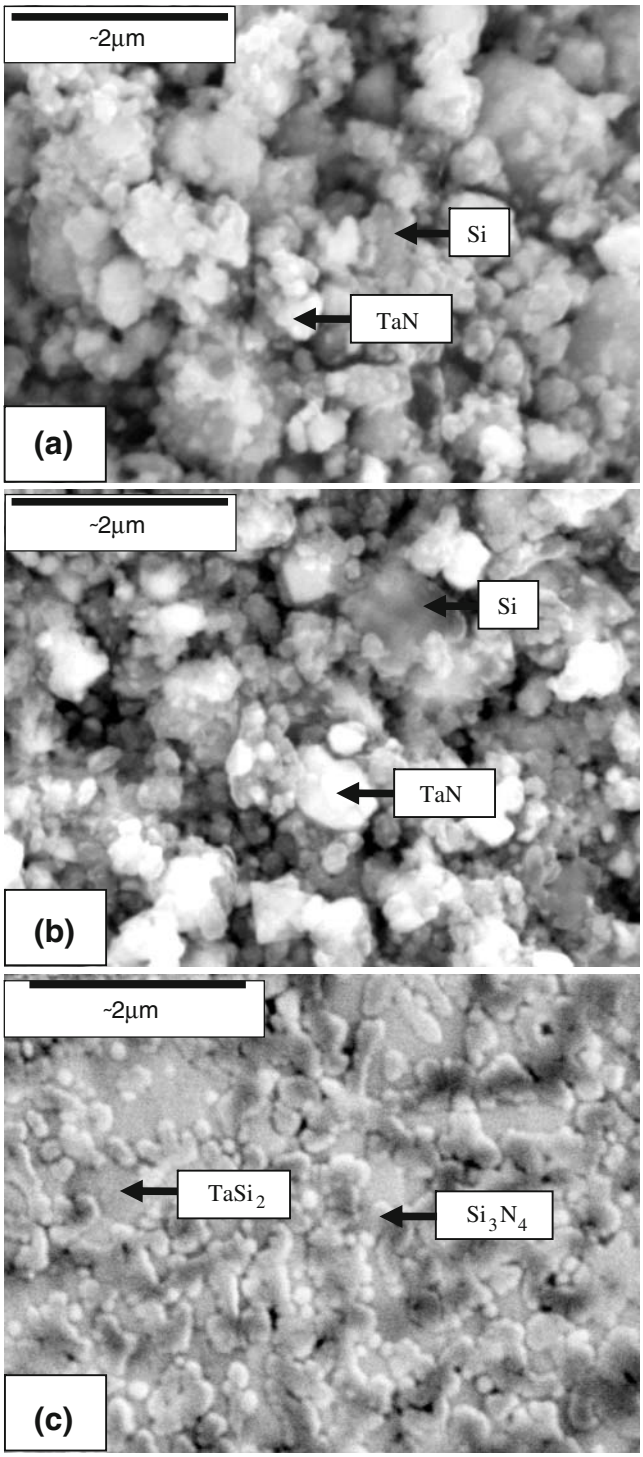

Fig. 6 Scanning electron microscope images of 4TaN+11Si system: (**a**) after milling (**b**) heating at 950 °C before combustion synthesis and (**c**) heating at 1100 °C after combustion synthesis

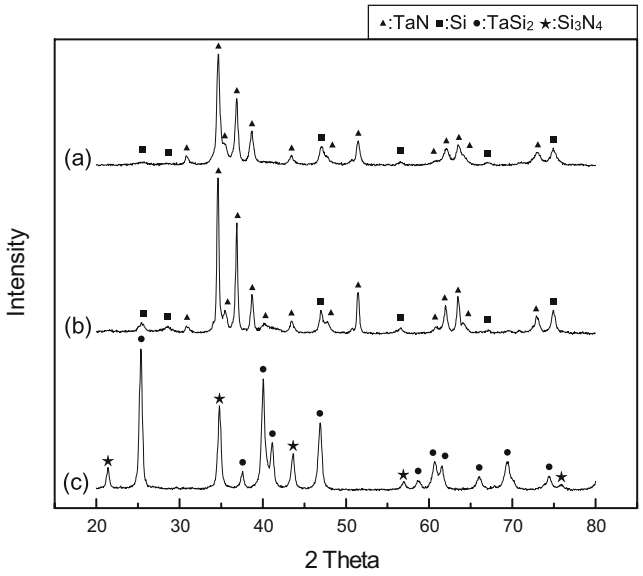

Fig. 7 XRD patterns of the 4TaN + 11Si system: (**a**) after milling (**b**) heating at 950 °C before combustion synthesis and (**c**) heating at 1100 °C after combustion synthesis

ary electron) images of (a) powder after milling, (b) sample heated to 950 °C and (c) sample heated to 1100 °C, respectively. Figures 6(a) and (b) show the presence of the reactants as separate phases. X-ray diffraction results shown in Fig. 7(a) and (b) exhibit only peaks pertaining to the reactants of TaN and Si. However, when the temperature was raised to 1100 °C, the starting powders react and then form highly dense products. SEM image of an etched surface of the samples heated to 1100 °C under a pressure of 60 MPa is shown in Fig. 6(c). A complete reaction between TaN and Si took place under these conditions. X-ray diffraction analyses of this sample showed peaks of only $TaSi_2$ and Si_3N_4, as indicated in Fig. 7(c). The abrupt increase in the shrinkage displacement at the ignition temperature is due to the increase in density as a result of molar volume change associated with the formation of $4TaSi_2$–Si_3N_4 from the reactants (TaN and Si) and the consolidation of the product. It should be recalled that the measured temperatures are those of the surface of the die and are, therefore, likely to be different than the values in the middle of the sample. Thus, the onset of the reaction to form the composite (and the concomitant rapid shrinkage) may be at a higher temperature than the observed value of 950 °C

The average grain sizes of $TaSi_2$ and Si_3N_4 calculated by the Stoke–Wilson's formula [29] were about 80 and 60 nm. The Si_3N_4 particles were well distributed in matrix, as can bee seen from the SEM image, Fig. 6(c).

Vickers hardness measurements were made on polished sections of the $TaSi_2$–Si_3N_4 composite using a 10 kg load and 15 s dwell time. The calculated hardness value, based on an average of five measurements, of the $TaSi_2$–Si_3N_4 composite is 1,403±26 kg/mm^2. Indentations with large enough loads produced median cracks around the indent. From the length of these cracks, fracture toughness values can be determined using two expressions. The first expression, proposed by Anstis et al. [30] is

$$K_{IC} = 0.016(E/H)^{1/2} \cdot P/C^{3/2} \quad (2)$$

where E is Young's modulus, H the indentation hardness, P the indentation load, and C the trace length of the crack measured from the center of the indentation, the modulus was estimated by the mixtures rule of the 0.129 volume fraction of Si_3N_4 and the 0.871 volume fraction of $TaSi_2$ using $E(Si_3N_4)$=308 GPa [31] and $E(TaSi_2)$=357 GPa [5]. The second expression, proposed by Niihara et al. [32, 33], is

$$K_{IC} = 0.023(c/a)^{-3/2} \cdot H_v \cdot a^{1/2} \quad (3)$$

where c is the trace length of the crack measured from the center of the indentation, a the half of average length of two indent diagonals, and H_v the hardness.

As in the case of hardness values, the toughness values were derived from the average of five measurements. The

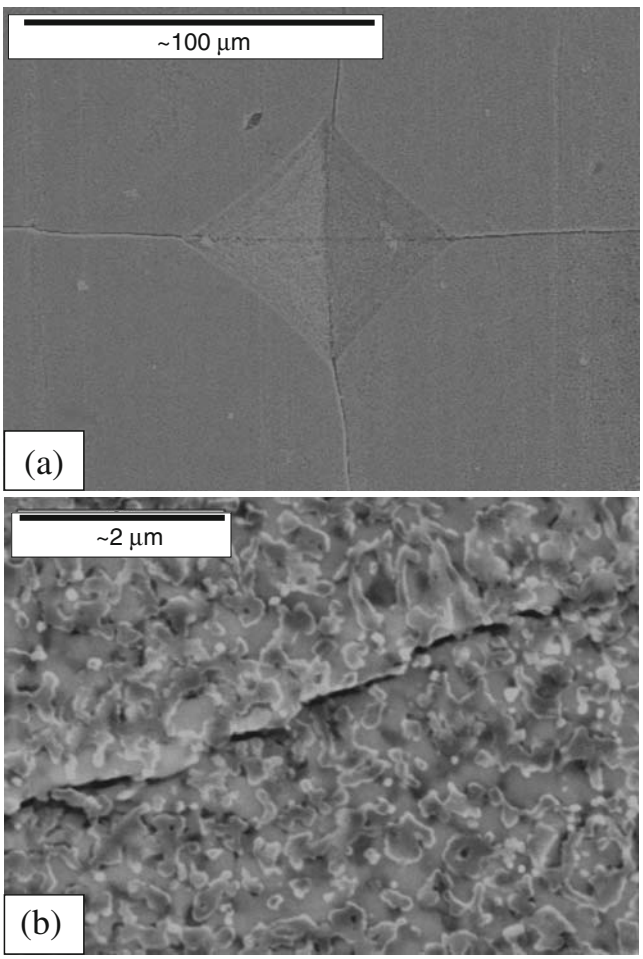

Fig. 8 (**a**) Vickers hardness indentation and (**b**) median crack propagating of $4TaSi_2$–Si_3N_4 composite

toughness values obtained by the two methods of calculation are 2.9±0.3 and 3.4±0.3 MPa·$m^{1/2}$, respectively.

A typical indentation pattern for the 4$TaSi_2$–Si_3N_4 composite is shown in Fig. 8(a). Typically, one to three additional cracks were observed to propagate from the indentation corner. Higher magnification view of the indentation median crack in the composite is shown in Fig. 8(b). This shows the crack propagates along phase boundary of $TaSi_2$ and Si_3N_4.

Although the absence of reported values for hardness and toughness on $TaSi_2$–Si_3N_4 precludes making direct comparison to the results obtained in this work to show the influence of grain size, we can evaluate the mechanical properties from the analogous metal silicide–Si_3N_4 composite system. For example, Murakami et al. have reported that the addition of Si_3N_4 to $NbSi_2$ or Nb_5Si_3 matrix increases the microvickers hardness [17]. We may analogy that the $TaSi_2$–Si_3N_4 composite may show lower hardness compared to Si_3N_4. The further study, however, may be necessary to verify the effect of grain size and the volume fraction of each component on mechanical properties in the $TaSi_2$–Si_3N_4 composite system.

4 Summary

Using the high-frequency induction-heated combustion method, the simultaneous synthesis and densification of nanocrystalline 4$TaSi_2$–Si_3N_4 composite was accomplished using powders of TaN and Si. Complete synthesis and densification can be achieved in one step within 1 min. The relative density of the composite was 99% under an applied pressure of 60 MPa and the induced current. The average grain sizes of $TaSi_2$ and Si_3N_4 phases in the composite were about 80 and 60 nm, respectively. The average hardness and fracture toughness values obtained were 1,403 kg/mm^2 and 3.4 MPa·$m^{1/2}$, respectively.

References

1. A.K. Vasudevan, J.J. Petrovic, J. Mater. Sci. Eng **A155**, 259 (1992) doi:10.1016/0921-5093(92)90308-N
2. G.J. Fan, M.X. Quan, Z.Q. Hu, J. Eckert, L. Schulz, Scripta Mater **41**, 1147 (1999) doi:10.1016/S1359-6462(99)00285-7
3. H. Okamoto, *Phase diagrams for binary alloys* (ASM international, 2000), pp 735
4. O. Knacke, O. Kubaschewski, K. Hesselmann, Springer-Verlag, 1973 (1991)
5. F. Chu, M. Lei, S.A. Maloy, J.J. Petrovic, T.E. Mitchell, Acta mater **44**, 3035 (1966) doi:10.1016/1359-6454(95)00442-4
6. G. Sauthoff, *Intermetallics* (VCH Publishers, New York, 1995)
7. Y. Ohya, M.J. Hoffmann, G. Petzow, J. Mater. Sci. Lett **12**, 149 (1993) doi:10.1007/BF00819942
8. J. Qian, L.L. Daemen, Y. Zhao, Diam. & Related Mater **14**, 1669 (2005) doi:10.1016/j.diamond.2005.06.007
9. B.W. Lin, T. Iseki, Br. Ceram. Trans. J **91**, 1 (1992)
10. Y. Ohya, M.J. Hoffmann, G. Petzow, J. Am. Ceram. Soc **75**, 2479 (1992) doi:10.1111/j.1151-2916.1992.tb05600.x
11. S.K. Bhaumik, C. Divakar, A.K. Singh, G.S. Upadhyaya, J. Mater. Sci. Eng **A279**, 275 (2000) doi:10.1016/S0921-5093(99)00217-8
12. D.K. Jang, R. Abbaschian, Kor. J. Mater. Res **9**, 92 (1999)
13. H. Zhang, P. Chen, M. Wang, X. Liu, Rare Metals **21**, 304 (2002)
14. D.Y. Oh, H.C. Kim, J.K. Yoon, I.J. Shon, Alloys & Compounds **395**, 174 (2005) doi:10.1016/j.jallcom.2004.10.072
15. W. Dressler, R. Riedel, Int. J. Refract. Met. Hard Mater **15**, 13 (1997) doi:10.1016/S0263-4368(96)00046-7
16. S.P. Taguchi, S. Ribeiro, J. Mater. Proce. Tech **147**, 336 (2004) doi:10.1016/j.jmatprotec.2004.01.003
17. T. Murakami, S. Sasaki, K. Ichikawa, A. Kitahara, Intermetallics **9**, 621 (2001) doi:10.1016/S0966-9795(01)00042-5
18. K. Bhattacharya, J.J. Petrovic, J. Am. Ceram. Soc **74**, 2700 (1991) doi:10.1111/j.1151-2916.1991.tb06828.x
19. Y. Luo, S. Li, W. Pan, L. Li, Mater. Lett **58**, 150 (2003) doi:10.1016/S0167-577X(03)00434-8
20. Z.A. Munir, I.J. Shon, K. Yamazaki, U. S. Patent No. **5**,794,113 (1998)
21. I.J. Shon, Z.A. Munir, K. Yamazaki, K. Shoda, J. Am. Ceram. Soc **79**, 1875 (1996) doi:10.1111/j.1151-2916.1996.tb08008.x
22. I.J. Shon, H.C. Kim, D.H. Rho, Z.A. Munir, Mater. Sci. Eng **A269**, 129 (1999) doi:10.1016/S0921-5093(99)00131-8
23. I.J. Shon, D.H. Rho, H.C. Kim, Z.A. Munir, J. Alloys & Compounds **322**, 120 (2001) doi:10.1016/S0925-8388(01)01167-7
24. I.J. Shon, D.H. Rho, H.C. Kim, Met. & Mater **6**, 533 (2000)
25. C.D. Park, H.C. Kim, I.J. Shon, Z.A. Munir, J. Am. Ceram. Soc **85**, 2670 (2002) doi:10.1111/j.1151-2916.2002.tb00492.x
26. H.C. Kim, D.Y. Oh, I.J. Shon, Int. J. Refrac. Met. & Hard Mater **22**, 41 (2004) doi:10.1016/j.ijrmhm.2003.12.002
27. H.C. Kim, D.Y. Oh, J. Guojian, I.J. Shon, Mater. Sci. Eng **A368**, 10 (2004) doi:10.1016/j.msea.2003.08.105
28. D.Y. Oh, H.C. Kim, J.K. Yoon, I.J. Shon, J. Alloys & Compounds **395**, 270 (2005) doi:10.1016/j.jallcom.2004.05.069
29. F.L. Zhang, C.Y. Wang, M. Zhu, Scripta Mater **49**, 1123 (2003) doi:10.1016/j.scriptamat.2003.08.009
30. G.R. Anstis, P. Chantikul, B.R. Lawn, D.B. Marshall, J. Am. Ceram. Soc **64**, 533 (1981) doi:10.1111/j.1151-2916.1981.tb10320.x
31. M. Lugovy, V. Slyunyayev, V. Subbotin, N. Orlovskaya, G. Gogotsi, Compos. Scie. and Tech **64**, 1947 (2004) doi:10.1016/j.compscitech.2004.02.007
32. N. Koichi, Ceramics **20**, 1218 (1985)
33. D.Y. Oh, H.C. Kim, J.K. Yoon, I.J. Shon, J. Alloys & Compound **395**, 174 (2005) doi:10.1016/j.jallcom.2004.10.072